Am J Transl Res 2017;9(3):1500-1508
www.ajtr.org /ISSN:1943-8141/AJTR0046437

Original Article

Expression of antisense of microRNA-26a-5p in mesenchymal stem cells increases their therapeutic effects against cirrhosis

Li Chen[1*], Wenhuan Zeng[2*], Bo Yang[3*], Xiang Cui[4], Cong Feng[1], Lili Wang[1], Hao Wang[5], Xuan Zhou[1], Peng Li[6], Faqin Lv[7], Tanshi Li[1]

Departments of [1]Emergency, [3]General Thoracic Surgery, [4]Orthopaedics, [5]Geriatric Cardiovascular, [6]Oncology Surgery, [7]Ultrasound, Chinese PLA General Hospital, 28 Fuxing Road, Beijing 100853, China; [2]Department of Emergency, Liuzhou General Hospital, 8 Wenchang Road, Liuzhou 545005, China. [*]Equal contributors and co-first authors.

Received December 12, 2016; Accepted February 15, 2017; Epub March 15, 2017; Published March 30, 2017

Abstract: Hepatocyte growth factor (HGF) is a potent mitogen for mature hepatocytes, and has been shown to prevent cirrhosis during liver regeneration. Transplantation of mesenchymal stem cells (MSCs) reduces the development of cirrhosis after liver injury. However, the production and secretion of transplanted MSCs in liver were not studied yet. Here we found that the MSCs expressed low levels of HGF protein, but surprisingly high levels of HGF mRNA. Further investigation using bioinformatics analyses and luciferase reporter assay showed that MSCs expressed high levels of microRNA-26a-5p (miR-26a-5p), which targeted 3'-UTR of HGF mRNA to inhibit its protein translation. In vivo, miR-26a-5p-depleted MSCs were transplanted into mice with carbon tetrachloride (CCl_4)-induced cirrhosis. We found that suppression of miR-26a-5p in MSCs further ameliorated the severity of liver fibrosis, reduced the portal hypertension and sodium retention, compared to transplantation of control MSCs. Hence, our study suggests that suppression of miR-26a-5p in MSCs may improve their therapeutic effects against cirrhosis through increasing HGF production.

Keywords: Mesenchymal stem cells (MSCs), cirrhosis, miR-26a-5p, hepatocyte growth factor (HGF)

Introduction

Infection by Hepatitis C virus often leads to development of chronic hepatitis, which may finalize into a prevalent hepatic fibrotic disease called cirrhosis [1-4]. Animal models have been used for studying the molecular mechanisms underlying the pathogenesis of cirrhosis, in which carbon tetrachloride (CCl_4) intraperitoneal injection has been widely applied due to low toxicity and high resemblance to human disease [5-10].

Hepatocyte growth factor (HGF) is a potent mitogen for mature hepatocytes, which promotes cell proliferation, suppresses apoptosis, and regulates cellular polarity and morphology [11-13]. HGF has been well documented to play critical roles in liver regeneration. Previous studies have applied HGF gene therapy in cirrhosis and achieved satisfactory results [14-16].

Transplantation of mesenchymal stem cells (MSCs) has therapeutic effects on a variety of diseases [17-25], including cirrhosis after liver injury [26-28]. However, approaches for augmentation of HGF production and secretion by MSCs have not been taken.

MicroRNAs (miRNAs) are small RNA species that range from 19 to 25 nucleotides in length [29-31]. Recent reports have shown that modification of miRNA levels in MSCs may improve their therapeutic potentials in treating Alzheimer's disease [32], and in preventing scarring after injury [33]. However, using miRNA-modified MSCs in prevention of cirrhosis has not been reported.

Recently, we showed that suppression of miR-219-5p activates keratinocyte growth factor to mitigate severity of experimental cirrhosis [34]. Here, we aimed to improve the effects of MSCs on cirrhosis protection through increasing HGF

production by MSCs via miRNA intervention. We found that the MSCs expressed low levels of HGF protein, but surprisingly high levels of HGF mRNA. Further investigation using bioinformatics analyses and luciferase reporter assay showed that MSCs expressed high levels of miR-26a-5p, which targeted 3'-UTR of HGF mRNA to inhibit its protein translation. In vivo, miR-26a-5p-depleted MSCs were transplanted into mice with carbon tetrachloride (CCl_4)-induced cirrhosis. We found that suppression of miR-26a-5p in MSCs further ameliorated the severity of liver fibrosis, reduced the portal hypertension and sodium retention, compared to transplantation of control MSCs.

Materials and methods

Experimental protocol approval and animal model establishment

All the experimental methods in the current study have been approved by the research committee at Chinese PLA General Hospital. All the experiments have been carried out in accordance with the guidelines from the research committee at Chinese PLA General Hospital. All mouse experiments were approved by the Institutional Animal Care and Use Committee at Chinese PLA General Hospital. Cirrhosis was induced in female C57BL/6 mice (Charles River Laboratories, China) at 10 weeks of age by CCl_4 intraperitoneal administration, as previously described [34]. Each experimental group contained 10 mice.

Isolation, culture and differentiation of mouse MSCs

Mouse bone marrow cells were isolated and cultured in DMEM culture medium (Dulbecco's Modified Eagle's Medium, Gibco, San Diego, CA, USA) containing inactivated 10% fetal bovine serum (FBS, Gibco), 3.7 g/l HEPES (N-2-hydroxyethylpiperazine-N'-2-ethane-sulphonic acid, Sigma-Aldrich, St. Louis, MO, USA), 1% 200 mmol/l L-glutamine 100× (Gibco) and 1% PSA (Gibco). After 72 hours' culture, the adherent MSCs were maintained until 80% confluence. After confirmation of MSC properties, a positive clone from the MSCs was picked up and subjected to chondrogenetic, osteogenic and adipogenic differentiation assays. For chondrogenetic induction, 2.5×10^5 MSCs were induced with 5 ml chondrogenetic induction medium containing 10 μg transforming growth factor β1 (TGFβ1, R&D System, Los Angeles, CA, USA), 50 μg insulin growth factor 1 (IGF-1, R&D System). The cells were maintained in the chondrogenetic induction medium for 14 days and then subjected to Alcian blue staining. For osteogenic induction, cells were digested and seeded onto a 24-well plate at a density of 10^4 cells/well, and then maintained in osteogenic induction medium containing 10 nmol/l Vitamin D3 (Sigma-Aldrich) and 10 mmol/l β-phosphoglycerol and 0.1 μmol/l DMSO for 14 days before subjected to Von kossa staining. For adipogenic induction, cells were digested and seeded onto a 24-well plate at a density of 10^4 cells/well, and then maintained in the adipogenic induction medium containing 0.5 mmol/l 3-isobutyl-1-methylxanthine (IBMX), 200 μmol/l indomethacin, 10 μmol/l insulin and 1 μmol/l DMSO for 14 days before subjected to Oil red O staining.

Plasmid and adeno-associated virus (AAV) preparation

Plasmids were successfully constructed using molecular cloning technology. Target sequences were inserted into pGL3-Basic vector (Promega, Beijing, China). Sequencing was performed to confirm the correct orientation of these new plasmids. Transfection was performed using Lipofectamine 2000 (Invitrogen, St. Louis, MO, USA). For AAV production, a pAAV-CMVp-RFP (red fluorescent protein) plasmid (Clontech, Mountain View, CA, USA), a packaging plasmid carrying the serotype 8 rep and cap genes, and a helper plasmid carrying the adenovirus helper functions (Applied Viromics, LLC. Fremont, CA, USA) were used to co-transfect Human Embryonic Kidney 293 cell line (HEK-293) to generate viruses. The viruses were purified using CsCl density centrifugation and then titered by a quantitative densitometric dot-blot assay. These viruses were used to transduce MSCs using a MOI of 50. The transduced cells expressed RFP, which allowed them to be purified by flow cytometry.

Luciferase-reporter activity assay

MiRNAs targets were predicted with the online tool from TargetScan, as described [35]. The candidates were analyzed for context+ score, which is the sum of site-type contribution, 3' pairing contribution, local AU contribution, posi-

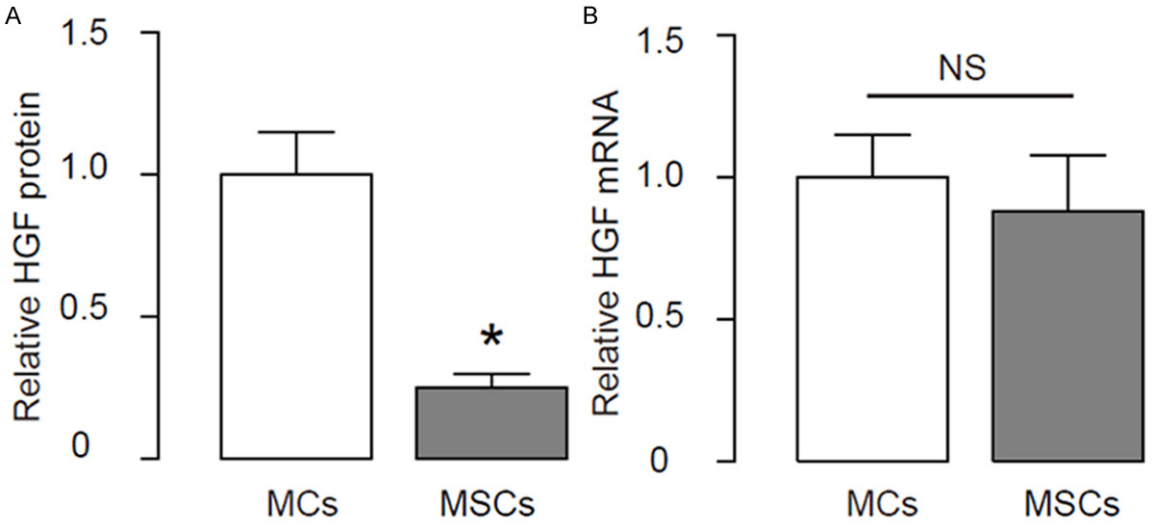

Figure 1. MSCs express low HGF protein but high HGF mRNA. MSCs were isolated from mouse bone marrow, and compared to vimentin-positive differentiated mesenchymal cells (MCs) for HGF expression. (A) ELISA for HGF protein (B) RT-qPCR for HGF mRNA. *: $P<0.05$. NS: non-significant. n=5. Statistics: one-way ANOVA with a Bonferroni correction.

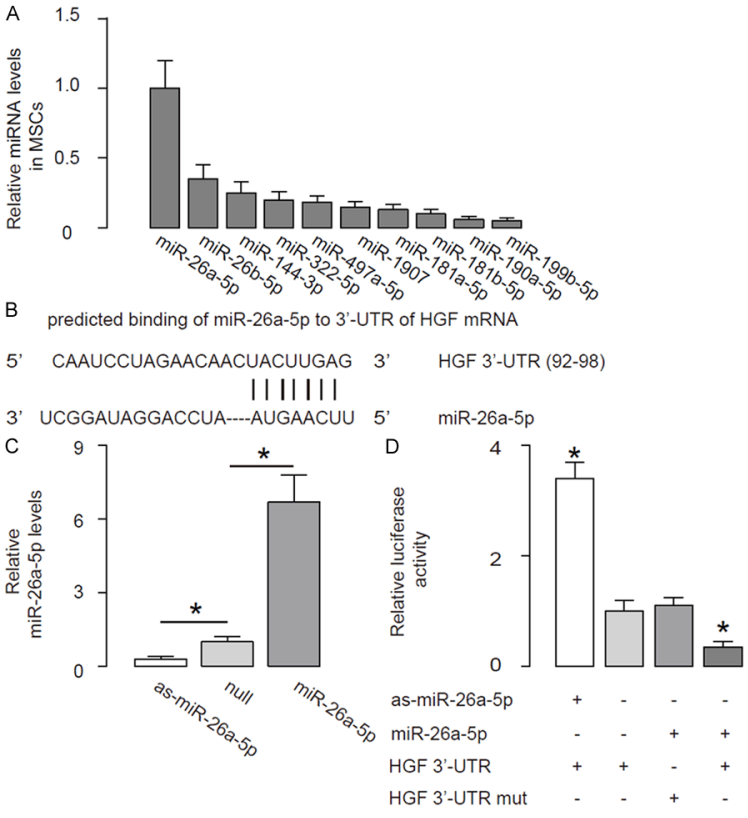

Figure 2. MiR-26a-5p targets 3'-UTR of HGF mRNA to inhibit its translation in MSCs. A. RT-qPCR for 10 miRNAs with detectable expression in MSCs. Among these 10 miRNAs, the expression of miR-26a-5p was the highest. B. Bioinformatics analyses showed that miR-26a-5p bound to 3'-UTR of HGF mRNA at 92nd-98th base site. C. MSCs were transfected with either miR-26a-5p, or antisense for miR-26a-5p (as-miR-26a-5p), or a null sequence as a control (null). RT-qPCR for HGF was performed. D. The intact 3'-UTR of HGF mRNA (HGF 3'-UTR) and a 3'-UTR with mutant at miR-26a-5p-binding site of HGF mRNA (HGF 3'-UTR mut) were cloned into luciferase reporter plasmids for co-transfection of MSCs with either as-miR-26a-5p/miR-26a-5p/null plasmids. Dual Luciferase-reporter assay was performed. *: $P<0.05$. NS: non-significant. n=5. Statistics: one-way ANOVA with a Bonferroni correction.

tion contribution, TA contribution and SPS contribution. The HGF 3'-UTR reporter plasmid (pRL-HGF) and the HGF 3'-UTR reporter plasmid with a mutant at miR-26a-5p binding site (pRL-HGF-mut) were purchased from Creative Biogene (Shirley, NY, USA). Cells were collected 36 hours after transfection for dual-luciferase reporter assay (Promega), according to the manufacturer's instructions.

Evaluation of liver fibrosis and function

Liver samples were fixed in 10% phosphate-buffered for-

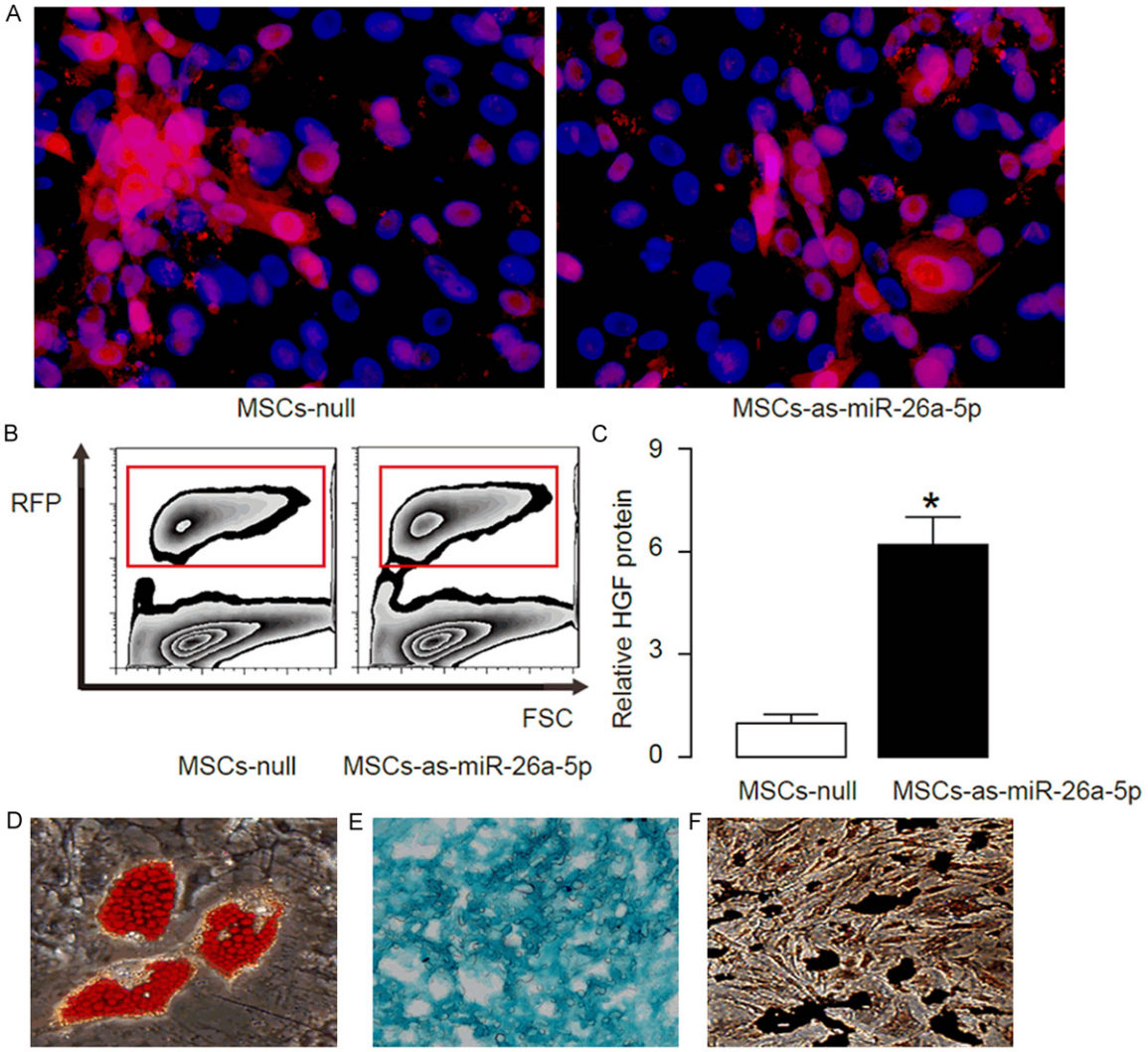

Figure 3. Preparation of miR-26a-5p-depleted MSCs. AAV carrying as-miR-26a-5p or control null was used to transduce MSCs. (A, B) The construct also contained a RFP reporter to allow visualization of the transduced cells in culture (A), and to allow purification of transduced cells by flow cytometry (B). (C) RT-qPCR for HGF in these cells. (D-F) A selected clone and confirmed its MSC phenotype using 3 differentiation assay. (D) Oil red O staining to evaluate adipogenic induction. (E) Alcian blue staining to evaluate chondrogenetic induction. (F) Von kossa staining to evaluate osteogenic induction. *: $P<0.05$. NS: non-significant. N=5. Statistics: one-way ANOVA with a Bonferroni correction.

malin, paraffin embedded, and then subjected to Sirius red staining for quantification, as has been described previously [34]. The urine sodium concentration (UNa) and the portal pressure assayed have been described previously [34].

Quantitative real-time PCR (RT-qPCR)

Total RNAs were extracted from liver or cultured cells with miRNeasy mini kit (Qiagen, Hilden, Germany) for cDNA synthesis. Quantitative real-time PCR (RT-qPCR) was performed in duplicates with QuantiTect SYBR Green PCR Kit (Qiagen). All primers were purchased from Qiagen. Data were collected and analyzed, using $2^{-\Delta\Delta Ct}$ method for quantification of the relative mRNA expression levels. Values of genes were first normalized against α-tubulin, and then compared to the experimental controls to get relative values.

ELISA

The concentration of HGF was determined by HGF ELISA Kit (R&D System, Los Angeles, CA, USA). ELISA was performed according to the instructions of the manufacturer.

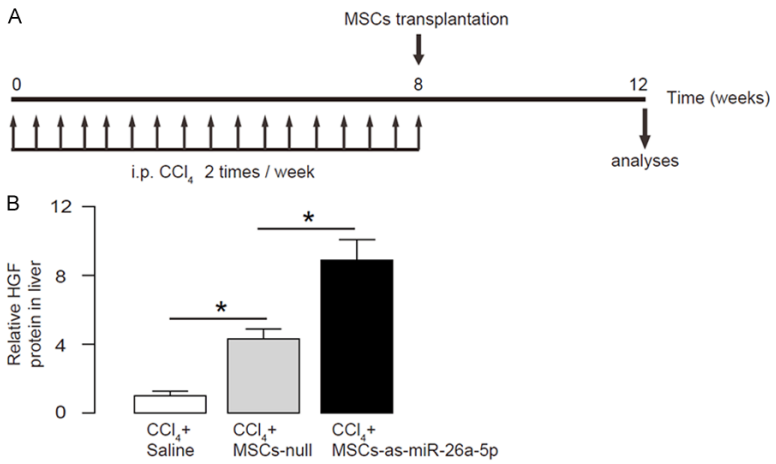

Figure 4. Depletion of miR-26a-5p in MSCs increases HGF levels in liver. A. Experimental schematic: CCl_4 was injected to induce cirrhosis in mice. After 8 weeks, the mice received transplantation of 10^6 MSCs-as-miR-26a-5p, or 10^6 MSCs-null, or saline, as 2 controls. The mice were then kept for another 4 weeks before analyses. B. Four weeks after transplantation, the HGF levels in the liver were analyzed by ELISA. *: $P<0.05$. NS: non-significant. N=10. Statistics: one-way ANOVA with a Bonferroni correction.

Statistical analysis

Statistical analyses were performed with SPSS 19.0 software (SSPS Inc., Chicago, IL, USA). All data were statistically analyzed using one-way ANOVA with a Bonferroni correction, followed by Fisher's Exact Test for comparison of two groups. All values are depicted as mean ± standard deviation, and are considered significant if $P<0.05$.

Results

MSCs express low HGF protein but high HGF mRNA

We isolated MSCs from mouse bone marrow, and examined the HGF levels in MSCs, compared to vimentin-positive differentiated mesenchymal cells (MCs) in mice. We found that MSCs expressed lower HGF protein (**Figure 1A**), but same level of HGF mRNA, compared to MCs (**Figure 1B**). These data suggest that the HGF expression in MSCs may be subjected to a post-transcriptional control, e.g. miRNAs.

MiR-26a-5p targets 3'-UTR of HGF mRNA to inhibit its translation in MSCs

Next, we examined the miRNAs that target HGF using performed bioinformatics analyses. We used a scoring system named "context++ score" to screen HGF-targeting miRNAs that have conserving binding sites [36] (Supplementary Table 1). From these candidates, there were 10 miRNAs that had detectable expression in MSCs (**Figure 2A**). Among these 10 miRNAs, the expression of miR-26a-5p was the highest (**Figure 2A**). Bioinformatics analyses showed that miR-26a-5p bound to 3'-UTR of HGF mRNA at 92nd-98th base site (**Figure 2B**). To determine if this binding of miR-26a-5p to HGF mRNA is functional, we transfected MSCs with either miR-26a-5p, or antisense for miR-26a-5p (as-miR-26a-5p), or a null sequence as a control (null). After the changes in miR-26a-5p levels were confirmed by RT-qPCR (**Figure 2C**), the intact 3'-UTR of HGF mRNA (HGF 3'-UTR), together with a 3'-UTR with mutant at miR-26a-5p-binding site of HGF mRNA (HGF 3'-UTR mut), was cloned into luciferase reporter plasmids for co-transfection of MSCs with either as-miR-26a-5p/null plasmids and HGF 3'-UTR or HGF 3'-UTR mut plasmids, or miR-26a-5p/null plasmids and HGF 3'-UTR or HGF 3'-UTR mut plasmids. The results from the dual Luciferase-reporter assay showed that miR-26a-5p may specifically target 3'-UTR of HGF mRNA to inhibit its translation in MSCs (**Figure 2D**).

Preparation of miR-26a-5p-depleted MSCs

Next, we prepared MSCs of permanent knockdown of miR-26a-5p in MSCs for examine its effects on cirrhosis prevention in vivo. Hence, we used AAV carrying as-miR-26a-5p or control null to transduce MSCs. The construct also contained a RFP reporter to allow visualization of the transduced cells in culture (**Figure 3A**), and to allow purification of transduced cells by flow cytometry (**Figure 3B**). Overexpression of as-miR-26a-5p in MSCs increased HGF levels by about 6 fold (**Figure 3C**). Before transplantation of as-miR-26a-5p-transduced MSCs into isogenic mice, we selected a clone and confirmed its MSC phenotype using 3 differentiation assay (**Figure 3D-F**).

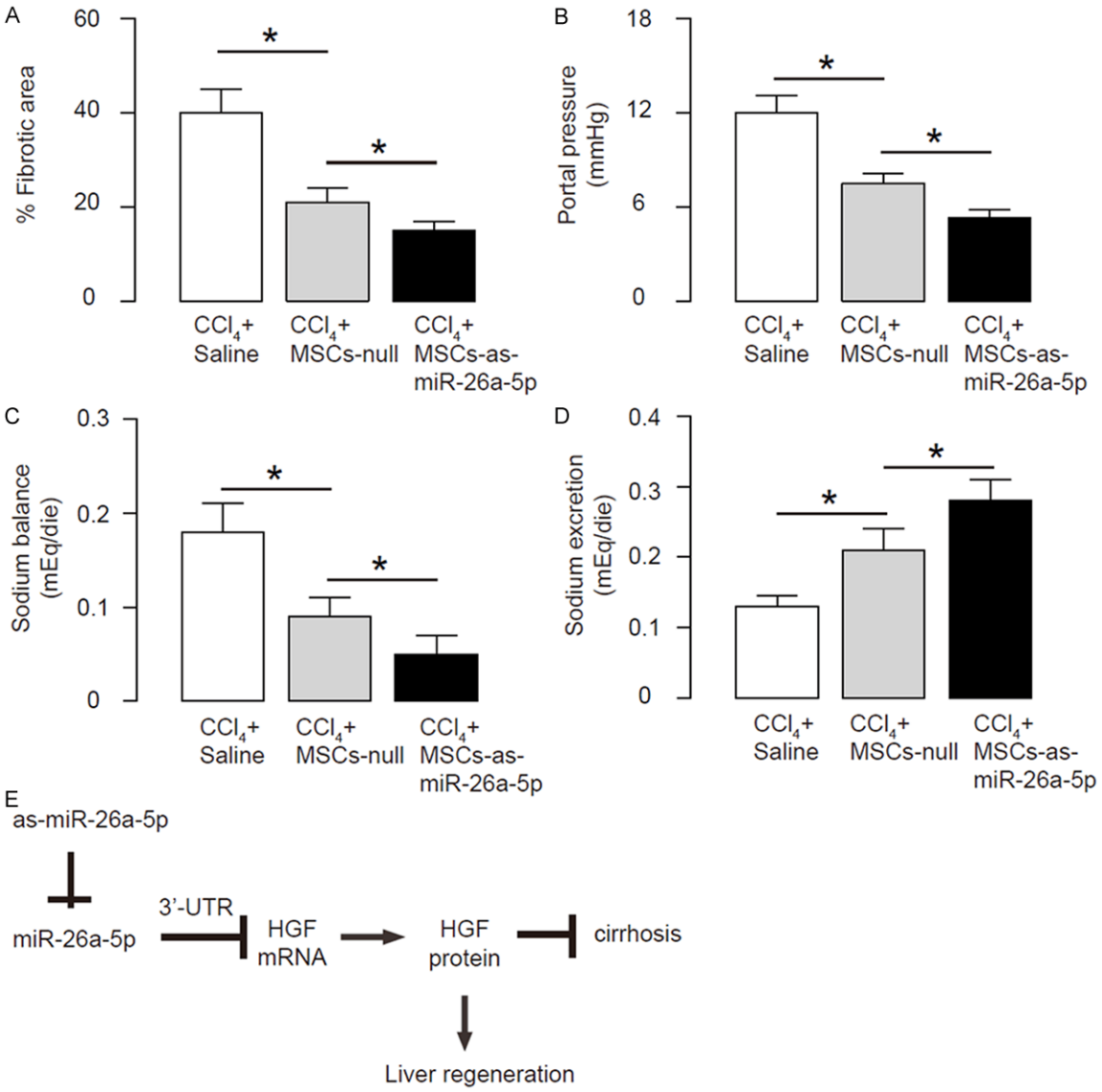

Figure 5. Depletion of miR-26a-5p in MSCs further attenuates severity of cirrhosis induced by CCl_4. A. The fibrotic area at sacrifice was evaluated after Sirius red staining, shown by the percentage of the fibrotic area. B. Portal pressure. C. Sodium balance. D. Sodium excretion. E. Schematic of the model: MiR-26a-5p expression in MSCs reduces HGF protein translation via direct binding to 3'-UTR of HGF mRNA. Suppression of miR-26a-5p in MSCs may improve their therapeutic effects against cirrhosis through increasing HGF production. *: $P<0.05$. n=10. Statistics: one-way ANOVA with a Bonferroni correction.

Depletion of miR-26a-5p in MSCs increases HGF levels in liver

Finally, we examined the effects of miR-26a-5p depletion in MSCs in vivo in a mouse model of cirrhosis. CCl_4 was injected to induce cirrhosis in mice. After 8 weeks, the mice received transplantation of 10^6 MSCs-as-miR-26a-5p, or 10^6 MSCs-null, or saline, as 2 controls. The mice were then kept for another 4 weeks before analyses (**Figure 4A**). Four weeks after transplantation, the HGF levels in the liver were analyzed, showing significant increases in the mice that received MSCs-as-miR-26a-5p, compared to those that received MSCs-null (**Figure 4B**).

Depletion of miR-26a-5p in MSCs further attenuates severity of cirrhosis induced by CCl_4

We found that transplantation of MSCs significantly decreased the percentage of the fibrotic area (**Figure 5A**). Portal hypertension and sodi-

um metabolism were also assessed, showing that transplantation of MSCs significantly decreased the portal pressure (**Figure 5B**), and significantly improved sodium balance (**Figure 5C**), probably through an increased sodium excretion (**Figure 5D**). Moreover, depletion of miR-26a-5p in MSCs further attenuates severity of cirrhosis induced by CCl_4 in all these settings (**Figure 5A-D**). Hence, our findings were summarized in a schematic, showing that suppression of miR-26a-5p in MSCs may further improve their therapeutic effects against cirrhosis via increasing HGF production (**Figure 5E**).

Discussion

Bone-marrow-derived MSCs have been widely used in treatment of fibrotic diseases. However, further enhancement of their power in tissue repair and regeneration could facilitate their applications. Thus, some recent reports have approached gene expression of MSCs through miRNA intervention. For example, Liu et al. suppressed miR-937 in MSCs, which increased the levels of BDNF production by MSCs to improve the therapeutic outcome in mouse model of Alzheimer's disease [19]. Sheng et al. showed that overexpression of miR-375 in MSCs significantly reduced the fibrosis in the scar region of the mice, through reduced secretion of TIMP-1 by MSCs [33]. These recent studies inspired to investigate if modified MSCs may have an improved therapeutic effects against cirrhosis.

Since HGF is a well-defined beneficial factor during liver regeneration, we selected it as a target in modifying MSCs. To our surprise, the mRNA and protein levels for HGF in MSCs were not comparable to those in MCs. These data suggest presence of post-transcriptional control in MSCs, since undifferentiated cells have distinct gene regulatory machinery from differentiated cells [37-39]. Thus, we think that the most effective approach to contradict a post-transcriptional control should be removal or dismissal of this control, rather than expression of additional mRNA for HGF, since presence of many cellular contradicting factor pairs may result in loss of biological efficiency and occurrence of disordering protein processing and ER stress [40].

Thus, we knocked down a HGF-antagonizing miRNA that is highly expressed in MSCs to achieve significant increases in HGF levels in MSCs. Compared to trophic factor infusion (here, HGF injection), a cell-based therapy has several advantages. First, the dose is regulated in a biological manner to cause less side effects. Second, the release of the factors by cells is more consistent than trophic factor infusion. To the best of our knowledge, this is the first study to show that the therapeutic effects of MSCs against cirrhosis could be improved through modification of a miRNA in MSCs. Further studies may address the miR-26-5p target genes other than HGF, to have a thorough estimation of the overall effects of miR-26-5p-depletion on the function of MSCs.

To summarize, the results from this study highly suggest that suppression of miR-26-5p in MSCs may increase the therapeutic potential of MSCs in preventing cirrhosis after liver injury.

SCI via augmentation of GDNF protein levels.

Acknowledgements

This study was supported by Youth Project of National Natural fund (No: 81400648), Beijing Scientific & Technologic Supernova Supportive Project (No: 15111000030000/XXJH2015-B100), Youth Culture Project of Chinese PLA (No: 13QNP171), Surface Project of Hainan Province Natural Fund (No: 20158315) and Clinical Advantage Supportive Programs of Chinese PLA General Hospital (No: 2012FC-TSYS-4028).

Disclosure of conflict of interest

None.

Address correspondence to: Faqin Lv, Department of Ultrasound, Chinese PLA General Hospital, 28 Fuxing Road, Beijing 100853, China. E-mail: lvjin8912@163.com; Tanshi Li, Department of Emergency, Chinese PLA General Hospital, 28 Fuxing Road, Beijing 100853, China. Tel: +861066937224; Fax: +861066937224; E-mail: lts302@yeah.net

References

[1] Hirschfield GM and Gershwin ME. The immunobiology and pathophysiology of primary biliary cirrhosis. Annu Rev Pathol 2013; 8: 303-330.

[2] Invernizzi P, Selmi C and Gershwin ME. Update on primary biliary cirrhosis. Dig Liver Dis 2010; 42: 401-408.

[3] Selmi C, Lleo A, Pasini S, Zuin M and Gershwin ME. Innate immunity and primary biliary cirrhosis. Curr Mol Med 2009; 9: 45-51.
[4] Tangkijvanich P and Yee HF Jr. Cirrhosis--can we reverse hepatic fibrosis? Eur J Surg Suppl 2002; 100-112.
[5] Selmi C, Meda F, Kasangian A, Invernizzi P, Tian Z, Lian Z, Podda M and Gershwin ME. Experimental evidence on the immunopathogenesis of primary biliary cirrhosis. Cell Mol Immunol 2010; 7: 1-10.
[6] Chuang YH, Ridgway WM, Ueno Y and Gershwin ME. Animal models of primary biliary cirrhosis. Clin Liver Dis 2008; 12: 333-347; ix.
[7] Wang J, Yang GX, Tsuneyama K, Gershwin ME, Ridgway WM and Leung PS. Animal models of primary biliary cirrhosis. Semin Liver Dis 2014; 34: 285-296.
[8] Leung PS, Yang GX, Dhirapong A, Tsuneyama K, Ridgway WM and Gershwin ME. Animal models of primary biliary cirrhosis: materials and methods. Methods Mol Biol 2012; 900: 291-316.
[9] Tsuneyama K, Moritoki Y, Kikuchi K and Nakanuma Y. Pathological features of new animal models for primary biliary cirrhosis. Int J Hepatol 2012; 2012: 403954.
[10] Concepcion AR and Medina JF. Approaches to the pathogenesis of primary biliary cirrhosis through animal models. Clin Res Hepatol Gastroenterol 2012; 36: 21-28.
[11] Abdelazim SA, Darwish HA, Ali SA, Rizk MZ and Kadry MO. Potential antifibrotic and angiostatic impact of idebenone, carnosine and vitamin E in nano-sized titanium dioxide-induced liver injury. Cell Physiol Biochem 2015; 35: 2402-2411.
[12] Zhang X, Tan Z, Wang Y, Tang J, Jiang R, Hou J, Zhuo H, Wang X, Ji J, Qin X and Sun B. PTPRO-associated hepatic stellate cell activation plays a critical role in liver fibrosis. Cell Physiol Biochem 2015; 35: 885-898.
[13] Guo JR, Li W, Wu Y, Wu LQ, Li X, Guo YF, Zheng XH, Lian XL, Huang HF and Chen YZ. Hepatocyte growth factor promotes proliferation, invasion, and metastasis of myeloid leukemia cells through PI3K-AKT and MAPK/ERK signaling pathway. Am J Transl Res 2016; 8: 3630-3644.
[14] Chen H, Xia R, Li Z, Zhang L, Xia C, Ai H, Yang Z and Guo Y. Mesenchymal stem cells combined with hepatocyte growth factor therapy for attenuating ischaemic myocardial fibrosis: assessment using multimodal molecular imaging. Sci Rep 2016; 6: 33700.
[15] Li S, Lv YF, Su HQ, Zhang QN, Wang LR and Hao ZM. A virus-like particle-based connective tissue growth factor vaccine suppresses carbon tetrachloride-induced hepatic fibrosis in mice. Sci Rep 2016; 6: 32155.
[16] Park M, Kim YH, Woo SY, Lee HJ, Yu Y, Kim HS, Park YS, Jo I, Park JW, Jung SC, Lee H, Jeong B and Ryu KH. Tonsil-derived mesenchymal stem cells ameliorate CCl4-induced liver fibrosis in mice via autophagy activation. Sci Rep 2015; 5: 8616.
[17] Li B, Shao Q, Ji D, Li F and Chen G. Mesenchymal stem cells mitigate cirrhosis through BMP7. Cell Physiol Biochem 2015; 35: 433-440.
[18] Liu W, Zhang S, Gu S, Sang L and Dai C. Mesenchymal stem cells recruit macrophages to alleviate experimental colitis through TGFbeta1. Cell Physiol Biochem 2015; 35: 858-865.
[19] Liu Z, Wang C, Wang X and Xu S. Therapeutic effects of transplantation of as-MiR-937-expressing mesenchymal stem cells in murine model of Alzheimer's disease. Cell Physiol Biochem 2015; 37: 321-330.
[20] Zhang J, Wu Y, Chen A and Zhao Q. Mesenchymal stem cells promote cardiac muscle repair via enhanced neovascularization. Cell Physiol Biochem 2015; 35: 1219-1229.
[21] Song X, Xie S, Lu K and Wang C. Mesenchymal stem cells alleviate experimental asthma by inducing polarization of alveolar macrophages. Inflammation 2015; 38: 485-492.
[22] Cao X, Han ZB, Zhao H and Liu Q. Transplantation of mesenchymal stem cells recruits trophic macrophages to induce pancreatic beta cell regeneration in diabetic mice. Int J Biochem Cell Biol 2014; 53: 372-379.
[23] Wang M, Zhang G, Wang Y, Liu T, Zhang Y, An Y and Li Y. Crosstalk of mesenchymal stem cells and macrophages promotes cardiac muscle repair. Int J Biochem Cell Biol 2015; 58: 53-61.
[24] Liu FB, Lin Q and Liu ZW. A study on the role of apoptotic human umbilical cord mesenchymal stem cells in bleomycin-induced acute lung injury in rat models. Eur Rev Med Pharmacol Sci 2016; 20: 969-982.
[25] Sun TJ, Tao R, Han YQ, Xu G, Liu J and Han YF. Wnt3a promotes human umbilical cord mesenchymal stem cells to differentiate into epidermal-like cells. Eur Rev Med Pharmacol Sci 2015; 19: 86-91.
[26] Zhang Z, Lin H, Shi M, Xu R, Fu J, Lv J, Chen L, Lv S, Li Y, Yu S, Geng H, Jin L, Lau GK and Wang FS. Human umbilical cord mesenchymal stem cells improve liver function and ascites in decompensated liver cirrhosis patients. J Gastroenterol Hepatol 2012; 27 Suppl 2: 112-120.
[27] Jung KH, Uhm YK, Lim YJ and Yim SV. Human umbilical cord blood-derived mesenchymal stem cells improve glucose homeostasis in rats with liver cirrhosis. Int J Oncol 2011; 39: 137-143.
[28] Puglisi MA, Saulnier N, Piscaglia AC, Tondi P, Agnes S and Gasbarrini A. Adipose tissue-derived mesenchymal stem cells and hepatic dif-

ferentiation: old concepts and future perspectives. Eur Rev Med Pharmacol Sci 2011; 15: 355-364.
[29] Pant S, Hilton H and Burczynski ME. The multifaceted exosome: biogenesis, role in normal and aberrant cellular function, and frontiers for pharmacological and biomarker opportunities. Biochem Pharmacol 2012; 83: 1484-1494.
[30] O'Loughlin AJ, Woffindale CA and Wood MJ. Exosomes and the emerging field of exosome-based gene therapy. Curr Gene Ther 2012; 12: 262-274.
[31] Bobrie A, Colombo M, Raposo G and Thery C. Exosome secretion: molecular mechanisms and roles in immune responses. Traffic 2011; 12: 1659-1668.
[32] Kaul G, Huang J, Chatlapalli R, Ghosh K and Nagi A. Quality-by-design case study: investigation of the role of poloxamer in immediate-release tablets by experimental design and multivariate data analysis. AAPS PharmSciTech 2011; 12: 1064-1076.
[33] Sheng W, Feng ZH, Song Q, Niu HY and Miao GY. Modulation of mesenchymal stem cells with miR-375 to improve their therapeutic outcome during scar formation. Am J Transl Res 2016; 8: 2079-2087.
[34] Chen L, Cui X, Li P, Feng C, Wang L, Wang H, Zhou X, Yang B, Lv F and Li T. Suppression of MicroRNA-219-5p activates keratinocyte growth factor to mitigate severity of experimental cirrhosis. Cell Physiol Biochem 2016; 40: 253-262.
[35] Coronnello C and Benos PV. ComiR: combinatorial microRNA target prediction tool. Nucleic Acids Res 2013; 41: W159-164.
[36] Agarwal V, Bell GW, Nam JW and Bartel DP. Predicting effective microRNA target sites in mammalian mRNAs. Elife 2015; 4.
[37] Sieweke MH and Allen JE. Beyond stem cells: self-renewal of differentiated macrophages. Science 2013; 342: 1242974.
[38] Tobe BT, Hou J, Crain AM, Singec I, Snyder EY and Brill LM. Phosphoproteomic analysis: an emerging role in deciphering cellular signaling in human embryonic stem cells and their differentiated derivatives. Stem Cell Rev 2012; 8: 16-31.
[39] Owens DM and Watt FM. Contribution of stem cells and differentiated cells to epidermal tumours. Nat Rev Cancer 2003; 3: 444-451.
[40] Rainbolt TK, Saunders JM and Wiseman RL. Stress-responsive regulation of mitochondria through the ER unfolded protein response. Trends Endocrinol Metab 2014; 25: 528-537.

Supplementary Table 1. Prediction of HGF-binding miRNAs by Bioinformatics

miRNA	Position in the UTR	Seed match	Context++ score
mmu-miR-199b-5p	2453-2460	8mer	-0.47
mmu-miR-199a-5p	2453-2460	8 mer	-0.47
mmu-miR-497a-5p	307-313	7mer-m8	-0.25
mmu-miR-6353	307-313	7mer-m8	-0.25
mmu-miR-15a-5p	307-313	7mer-m8	-0.24
mmu-miR-195b	307-313	7mer-m8	-0.24
mmu-miR-195a-5p	307-313	7mer-m8	-0.24
mmu-miR-16-5p	307-313	7mer-m8	-0.24
mmu-miR-6419	307-313	7mer-m8	-0.24
mmu-miR-15b-5p	307-313	7mer-m8	-0.24
mmu-miR-322-5p	307-313	7mer-m8	-0.23
mmu-miR-6342	307-313	7mer-m8	-0.23
mmu-miR-26b-5p	226-233	8mer	-0.22
mmu-miR-497b	3191-3197	7mer-m8	-0.22
mmu-miR-26a-5p	226-233	8 mer	-0.2
mmu-miR-1907	307-313	7mer-m8	-0.18
mmu-miR-140-3p.2	3191-3197	7mer-m8	-0.18
mmu-miR-128-3p	3189-3195	7mer-m8	-0.17
mmu-miR-19b-3p	3054-3061	8mer	-0.15
mmu-miR-19a-3p	3054-3061	8mer	-0.15
mmu-miR-6539	3189-3195	7mer-m8	-0.13
mmu-miR-101a-3p.1	2545-2552	8mer	-0.1
mmu-miR-190b-5p	210-216	7mer-m8	-0.09
mmu-miR-181d-5p	2558-2564	7mer-m8	-0.09
mmu-miR-181a-5p	2558-2564	7mer-m8	-0.08
mmu-miR-181b-5p	2558-2564	7mer-m8	-0.08
mmu-miR-190a-5p	210-216	7mer-m8	-0.07
mmu-miR-181c-5p	2558-2564	7mer-m8	-0.07
mmu-miR-381-3p	3203-3209	7mer-m8	-0.06
mmu-miR-539-3p	3203-3209	7mer-m8	-0.06
mmu-miR-374c-5p	3205-3211	7mer-m8	-0.06
mmu-miR-26a-5p	92-98	7mer-m8	-0.05
mmu-miR-26b-5p	92-98	7mer-m8	-0.05
mmu-miR-144-3p	3095-3101	7mer-m8	-0.05
mmu-miR-369-3p	3206-3213	8mer	-0.04
mmu-miR-335-5p	2409-2415	7mer-m8	-0.03
mmu-miR-653-5p	2429-2436	8mer	-0.03
mmu-miR-144-3p	2546-2552	7mer-1A	-0.03
mmu-miR-1224-5p	2369-2375	7mer-m8	-0.02
mmu-miR-101b-3p.1	2546-2552	7mer-m8	-0.02
mmu-miR-101a-3p.2	2546-2552	7mer-m8	-0.02
mmu-miR-101b-3p.2	2546-2552	7mer-m8	-0.02
mmu-miR-543-3p	2559-2565	7mer-m8	-0.02
mmu-miR-590-5p	3139-3145	7mer-m8	-0.02
mmu-miR-21c	3139-3145	7mer-m8	-0.02
mmu-miR-21a-5p	3139-3145	7mer-m8	-0.02

The context++ score for a specific site has been recently developed as an improved quantitative model of canonical targeting, using a compendium of experimental datasets to minimize confounding biases. The context++ score considers site type and another 14 features to predict the most effectively targeted mRNAs, in which It drives the latest version of TargetScan (v7.0; targetscan.org), thereby providing a valuable resource for placing miRNAs into gene-regulatory networks. Predicted targets of each miRNA family are sorted by total context++ score. The representative miRNA is the miRNA in its family with the most favorable (lowest) total context++ score.